Contents lists available at ScienceDirect

Microelectronic Engineering

journal homepage: www.elsevier.com/locate/mee

Research paper

New serial resistance equations: Derivated from Cheungs' functions for the forward and reverse bias I

A. Korkut

Department of Physics, Faculty of Science, Yüzüncü Yıl University, Van, Turkey

A B S T R A C T

In this study, a group of new series resistance has been derived using Cheung functions. In contrast to the traditional approximation, new serial resistance formulae result in very exceptional value from the conventional serial resistance values for both cases, the forward bias and the reverse bias. These new serial resistance formulae exhibit a stable behavior. Besides, the relation between R_{Ns1}-I, R_{Ns2}-I, R_{Ns1}-V_{bi} and R_{Ns2}-V_{bi} could be shown easily. It is enough to take the current matching of the integer values of the built-in potential.

1. Introduction

The metal-semiconductor interface is essential for the electrical characteristics of diodes. Schottky diodes of (Ag, Cu)/n-Si/Al are the specimens for that work. The parameters of diodes are ideality factor (n_{IV}), barrier height (Φ_{BH}), Cheung functions (Ch1, Ch2) [1], built-in potential (V_{bi}), and serial resistance (R_s) [2]. Schottky diodes comprise four sections; Ohmic junction, base structure, depletion layer, and Schottky junction [3]. This study aims to determine how the primary characteristics of Schottky MS diodes vary by a serial resistance (R_s), obtained by a new method.

2. Materials and method

2.1. Experimental method

In this work, n-Si wafers with (100) orientation were used. It has a thickness of 450 μm and a resistivity of ρ = 1–10 Ω·cm. The samples were chemically cleaned from chemical and organic contaminants [4]. The samples were boiled for first 3 min in RCA (NH_4OH) and then in ($HCl + H_2O_2 + 6H_2O$). The samples were then etched in $HF:H_2O$(1:10) for 30 s and rinsed in the deionized water within ultrasonic vibration [4, 5]. The n-Si wafer was cut into two pieces (5 × 5 mm²). Later, the back side of these pieces of samples was formed by Ohmic contact through evaporation of the cleaned Al at the Torr pressure of 10^{-6} and at the temperature of 425 °C for 3 min in flowing N_2 gas. By doing so, the ohmic contact was formed for all samples. One of the samples was immediately inserted into the evaporation chamber, and Ag (5 N pure) evaporated onto front side Schottky contact at the 10^{-6} Torr pressure, which is the repeated process for Cu (5 N pure). Thus, we have fabricated Ag100%/n-Si/Al (D1; first diode), Cu100%/n-Si/Al (D2; second diode) as Schottky diodes (see Appendix Table A1).

The characteristics of Schottky diode were specified using ln(I)-V and C_s-V measurements for both cases of the forward bias (FB) and the reverse bias (RB), which were plotted for positive and negative voltage [2, 6, 7]. On the contrary to the traditional calculations, each parameter of the ideality factors (n_{FB} and n_{RB}) and the serial resistances (R_{s-FB} and R_{s-RB}) were calculated. It is seen that serial resistances R_{s-IV} obeyed to Cheung I equation using $H(I)_{Ch1}$–I plot for both cases [6, 7]. For the frequency of 250 kHz, the measurements of diodes (C_s-V and I-V) were made at the room temperature (300 °K) and in the dark environment.

2.2. Thermionic equation and new serial resistances

A diode is featured by ideality factor. According to thermionic emission theory, the characteristics of current-voltage in Schottky diode can be expressed in Eqs. (3)–(11). Current equation for non-ideal condition is given by

$$I = AR_n^* T^2 \exp\left(-\frac{e\Phi_{BH}}{kT}\right)\left[\exp\left(\frac{e(V - IR_s)}{nkT}\right)\right] \tag{1}$$

where n is the ideality factor, V the applied voltage, e the electron charge, R_s the series resistance, k the Boltzmann constant, T temperature in Kelvin, R_n^*, the Richardson constant (110 A/cm²·K² for n-type Si) [2, 3, 6–12], A the effective diode area (radius: 0.4 mm), and Φ_{BH} the effective barrier height.

$$V = \left(\frac{n_{if}kT}{e}\right)\ln\left(\frac{I}{AR_n^* T^2}\right) + n\Phi_{BH} + IR_S \tag{2}$$

and Cheung I formula (1) is

$$H_{Ch1}(I) = \frac{dV}{d(lnI)} = \left(\frac{n_{if\text{-}IV}kT}{e}\right) + IR_S \tag{3}$$

and Cheung II formula (1) is

$$H_{Ch2}(I) = V - \left(\frac{n_{if}kT}{e}\right)ln\left(\frac{I}{AR_n^*T^2}\right) = n_{if\text{-}Ch1}\Phi_{BH} + IR_S \tag{4}$$

with a simple reduction:

$$\beta_o = \left(\frac{n_{if}kT}{e}\right) \Rightarrow \beta_o = \left(\frac{\beta}{n_{if}}\right)^{-1}; \gamma_o = \frac{1}{AR_n^*T^2} \tag{5}$$

Eq. (5) could write in Eq. (2) as following

$$V = \beta_o ln(\gamma_o I) + n\Phi_{BH} + IR_S$$
$$V = \beta_o ln(I) + [\beta ln(\gamma_o) + n\Phi_{BH}] + IR_S \tag{6}$$

$$V = V(ln(I), I) \tag{7}$$

$$H_{Ch1} = \frac{\partial V}{\partial ln(I)} = \beta_o + IR_S; \quad H_{Ko3} = \frac{\partial V}{\partial I} = \frac{\beta_o}{I} + R_S \tag{8}$$

To express easily, let's restate the left equation as the right equation using H_{Ko3} in Eq. (8) and a new serial resistance obtains:

$$R_{Ns1} = H_{Ko3} - \frac{\beta_o}{I} = \frac{\partial V}{\partial I} - \frac{\beta_o}{I} \tag{9}$$

Henceforth, that new serial resistance will call first new serial resistance (R_{Ns1}) (or FNSR). If H_{Ko3} is multiplied by I (current)

$$\frac{\partial V}{\partial ln(I)} = I\frac{\partial V}{\partial I} \tag{10}$$

Eq. (10) obtains as a general equation. Eq. (10) takes the derivative to ln I and I

$$\frac{\partial^2 V}{\partial ln(I)^2} = I\frac{\partial V}{\partial I} + I\frac{\partial^2 V}{\partial I \times \partial ln(I)} \Rightarrow \frac{\partial^2 V}{\partial ln(I)^2} - I\frac{\partial V}{\partial I} - I\frac{\partial^2 V}{\partial I \times \partial ln(I)} = 0 \tag{11}$$

$$\frac{\partial^2 V}{\partial ln(I) \times \partial I} = \frac{\partial V}{\partial I} + I\frac{\partial^2 V}{\partial I^2} \Rightarrow \frac{\partial^2 V}{\partial I^2} + \frac{1}{I}\frac{\partial V}{\partial I} - \frac{1}{I}\frac{\partial^2 V}{\partial I \times \partial ln(I)} = 0 \tag{12}$$

Let's sum Eqs. (11) and (12). To prove physical parameters, they are transformed to mathematics parameters as follows; I = x and z = ln(x)

$$\frac{\partial^2 V}{\partial ln(x)^2} + \frac{\partial^2 V}{\partial x^2} - \frac{\partial V}{\partial I}\left(x - \frac{1}{x}\right) - \frac{\partial^2 V}{\partial I \times \partial ln(I)}\left(x + \frac{1}{x}\right) = 0 \tag{13}$$

$$\frac{\partial^2 V}{\partial z^2} + \frac{\partial^2 V}{\partial x^2} - \frac{\partial V}{\partial I}\left(x - \frac{1}{x}\right) - \frac{\partial^2 V}{\partial I \times \partial z}\left(x + \frac{1}{x}\right) = 0 \tag{14}$$

$$\frac{\partial z}{\partial x} = \frac{1}{x} \Rightarrow \frac{\partial^2 z}{\partial x^2} = -\frac{1}{x^2} \Rightarrow \frac{\partial z}{\partial ln(x)} = 1 \Rightarrow \frac{\partial^2 z}{\partial ln(x)^2} = 0 \tag{15}$$

$$\frac{\partial y}{\partial z} = \frac{\partial y}{\partial x}\frac{\partial x}{\partial z} = \frac{\partial y}{\partial x}\left(\frac{\partial x}{\partial z}\right)^{-1} = x\frac{\partial y}{\partial x} \tag{16}$$

$$\frac{\partial^2 V}{\partial x \times \partial z} = \frac{\partial}{\partial x}\left[x\frac{\partial y}{\partial x}\right] = \frac{\partial y}{\partial x} + x\frac{\partial^2 y}{\partial x^2} \tag{17}$$

$$\frac{\partial^2 y}{\partial z^2} = \frac{\partial}{\partial z}\left[\frac{\partial y}{\partial z}\right] = \frac{\partial}{\partial x}\left[\frac{\partial y}{\partial z}\right]\frac{\partial x}{\partial z} \Rightarrow \frac{\partial^2 y}{\partial z^2} = x\frac{\partial y}{\partial x} + x^2\frac{\partial^2 y}{\partial x^2} \tag{18}$$

Let's write Eqs. (15) and (18) in Eq. (14),

$$\left[x\frac{\partial y}{\partial x} + x^2\frac{\partial^2 y}{\partial x^2}\right] + \frac{\partial^2 y}{\partial x^2} - \frac{\partial y}{\partial x}\left(x - \frac{1}{x}\right) - \left[\frac{\partial y}{\partial x} + x\frac{\partial^2 y}{\partial x^2}\right]\left(x + \frac{1}{x}\right) = 0 \tag{19}$$

$$-x\frac{\partial y}{\partial x} = 0 \tag{20}$$

and then math parameters are re-transformed to physics parameter:

$$-I\frac{\partial V}{\partial I} = 0 \Rightarrow I\left[\frac{\beta_o}{I} + R_S\right] = 0 \Rightarrow \beta_o + IR_S = 0 \tag{21}$$

$$R_S = -\frac{\beta_o}{I} \Rightarrow R_S = -\left(\frac{nkT}{e}\right)\frac{1}{I} \tag{22}$$

and new serial resistance formula was obtained depending on ideality factor and current. Henceforth, R_S will be called second new serial resistance (R_{Ns2}) (or SNSR) for clarity.

Eq. (9) is rearranged using Eq. (22):

$$H_{Ko3} = R_{Ns1} - R_{Ns2} = \frac{\partial V}{\partial I} \tag{23}$$

A new equation is found between the first and the second serial resistance. Henceforth, H_{Ko3} is the difference between the new serial resistances (ΔR_{Ns}) (or DNSR).

2.3. How ideality factor obtain?

Ideality factors are found from ln I-V plot for both forward bias and reverse bias [2, 3, 6–10]. n_{FB} is the ideality factor in the case of forward bias. n_{RB} is the ideality factor in the case of reverse bias. The ideality factors are calculated using the following formula:

$$n_{IF} = \left(\frac{e}{kT}\right)\left(\frac{dV}{d(lnI)}\right) \tag{24}$$

The ideality factors are obtained from fitting lines in the case of forward bias and reverse bias (see Fig. 1a, b).

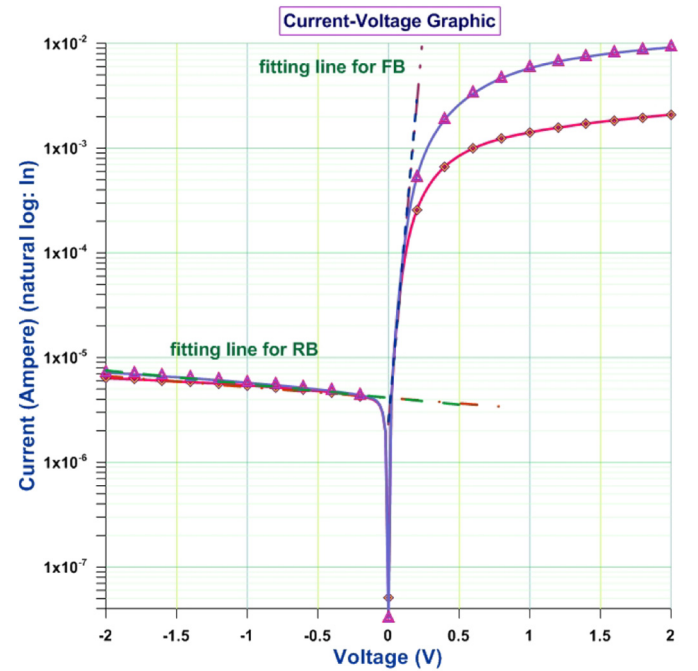### 2.4. H(I)-I Cheung I, II graphics

Cheung functions are like [1],

Fig. 1. a) Forward bias, and b) reverse bias in ln I - V graph, (diamond symbol is shows to the Cu/n-Si/Al diode, line-dot-line is shows to fitting line for Cu/n-Si/Al diode, triangle symbol is shows Ag/n-Si/Al diode, dash line shows to fitting line for Ag/n-Si/Al diode) (see for ideality factors and equation of the fittings values in Appendix Table A1).
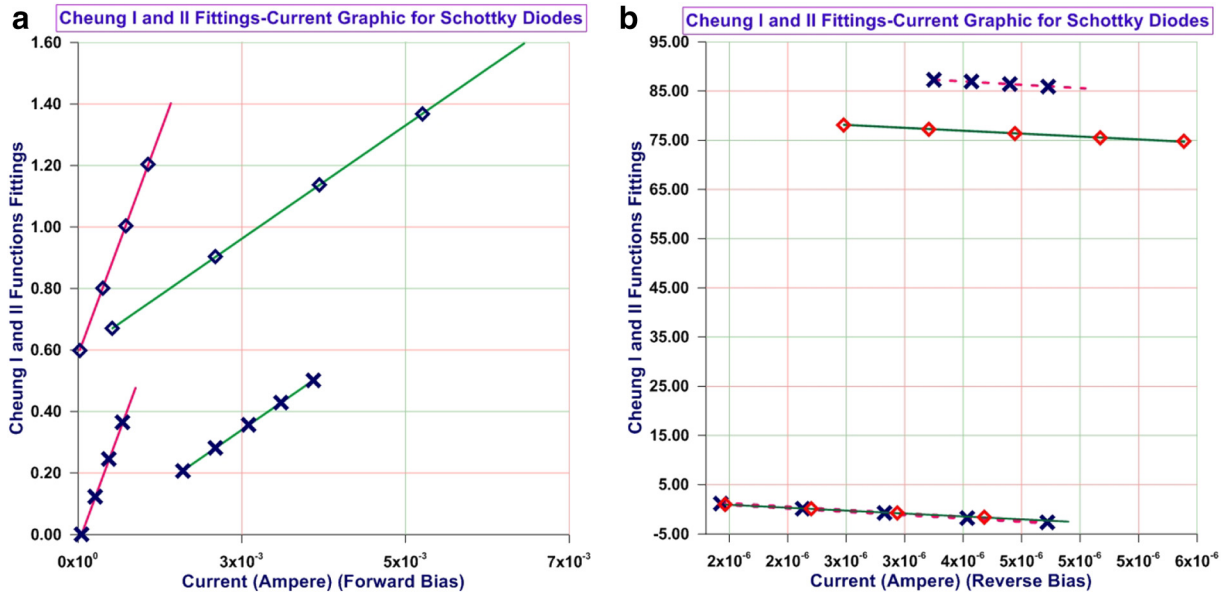
46

Fig. 2. a) Forward bias, H(I)$_{Ch1,Ch2}$-I graph for Cu/n-Si/Al (pink line), Ag/n-Si/Al (green line) Schottky diode (pink and green line show the Ch1 (cross symbol), Ch2 (diamond symbol) fittings), b) Reverse bias; H(I)$_{Ch1, Ch2}$-I graph for Cu/n-Si/Al (cross symbol), Ag/n-Si/Al (diamond symbol) Schottky diodes (pink and green line show the Ch1 (dash line), Ch2 (green line) fittings), (see Appendix Table A1). (For interpretation of the references to color in this figure legend, the reader is referred to the web version of this article.)

$$H(I)_{Ch1} = IR_s + n_{IV}kT/e; \quad H(I)_{Ch2} = IR_s + n_{Ch1}\Phi_{BH} \quad (25)$$

Fig. 2(a) and (b) shows Cheung I and II equation fittings in both cases of the Metal/n-Si/Al diodes for forward and reverse bias (see Appendix Table A1). As seen from Fig. 2(a) and (b), down-fittings belong to Ch1 functions and its slope gives the serial resistance (R$_{s-Ch1}$) and ideality factor (n$_{IF}$). Up-fittings, however, belong to Ch2, and its slope provides the serial resistance (R$_{s-Ch2}$) and the barrier height (Φ$_{BH}$). On the contrary to the traditional approximation, first time Ch2 was calculated in the case of reverse bias, and the fittings of Ch1 and Ch2 functions (for both diodes) have got a negative slope (see Fig. 2).

2.5. First new serial resistance approximation

Using Eq. (9) let us draw new serial resistance plots for both forward and reverse bias. In the case of forward bias, log R$_{Ns1}$-I is plotted, and it took its exponential fittings for D1 Schottky diode (in Fig. 3a). The exponential fitting equations resolve the matching current on V$_{bi}$ values (see Appendix Table A2). In the case of reverse bias, R$_{Ns1}$-I is plotted, and it took its linear fittings for two metal Schottky diodes (in Fig. 3b). The linear fitting equations resolve the matching current on V$_{bi}$ values (see Appendix Table A2). Thus, R$_{Ns1}$ is calculated for two Schottky diodes. The solutions for the Schottky diodes are seen in Appendix Table A1.

As can be seen above, we are making the exponential fitting of the diodes of Ag/n-Si/Al and Cu/n-Si/Al. The graph in Fig. 3a is semi-logarithmic that the vertical axis is logarithmic and the horizontal axis is linear while both in Fig. 3b are linear. The latter one shows negative values on the vertical axis. The data used here can be seen in Appendix
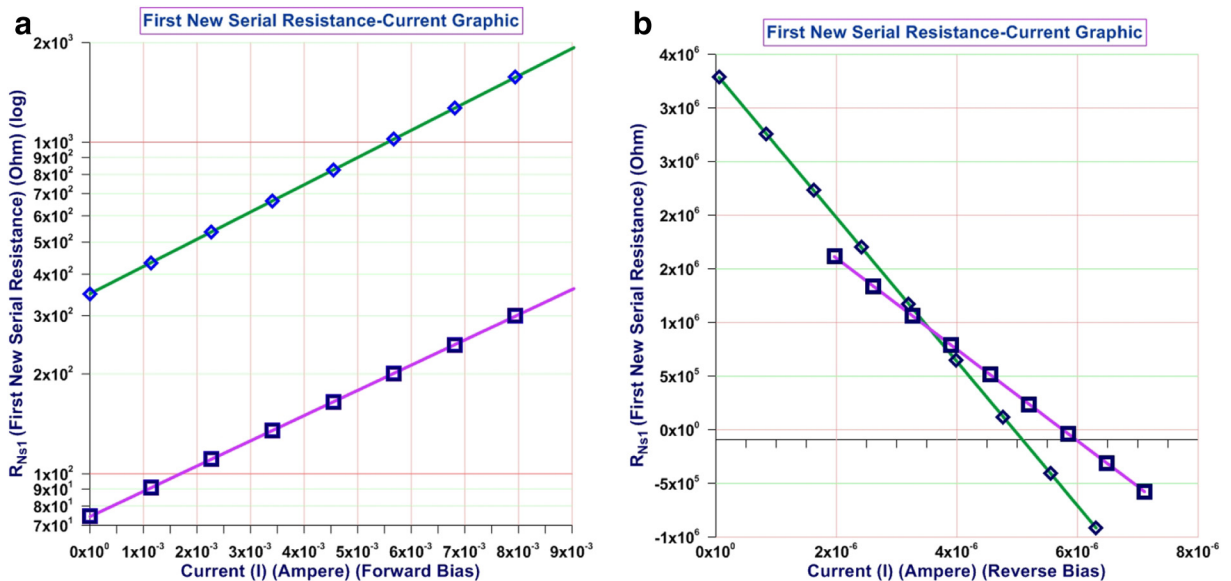

Fig. 3. R$_{Ns1}$-I versus current for Cu/n-Si/Al (green line), Ag/n-Si/Al (purple line) Schottky diodes in the cases of (a) forward bias, and (b) reverse bias. (For interpretation of the references to color in this figure legend, the reader is referred to the web version of this article.)
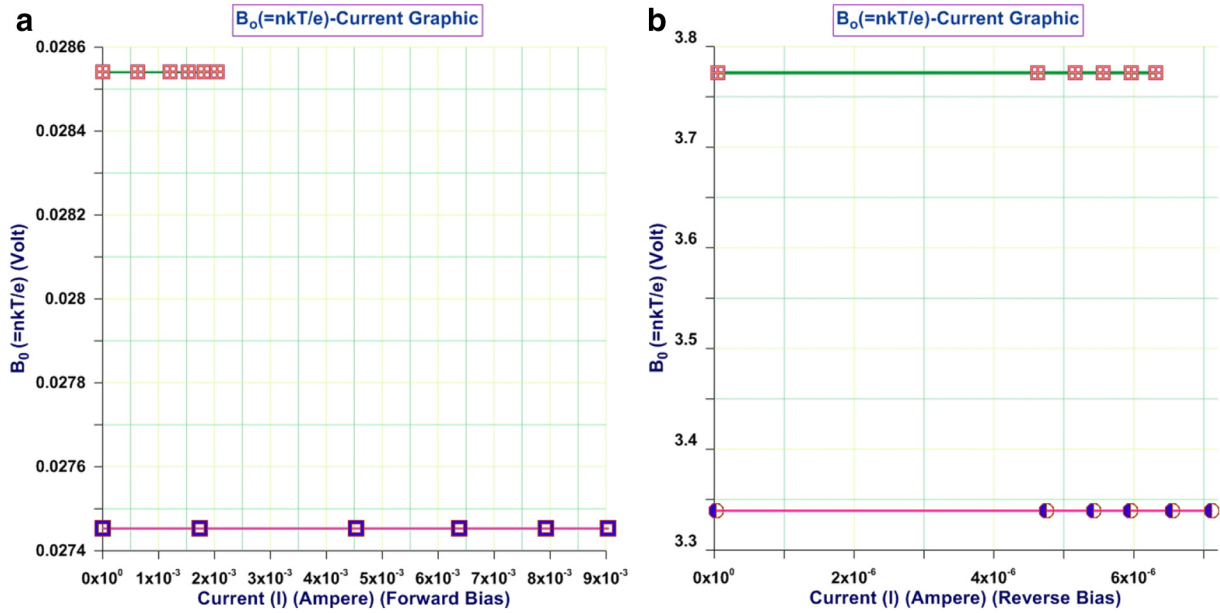
Fig. 4. a, b. The cases of forward bias and reverse bias B_0-I graphs for Cu/n-Si/Al (green line), Ag/n-Si/Al (pink line), Schottky diodes.

Table A2.

2.6. Correlation of the matching current and built-in potential

At this point, we argue that there is a relationship between the built-in potential and the current matching value to V_{bi}. The built-in potential values are V_{bi}, $2V_{bi}$, $3V_{bi}$, $4V_{bi}$, … and every V_{bi} has current matching value on the V_{bi}. The current matching value on V_{bi} is beneficial; otherwise, it will require further trials with too much data. The current matching values are given in Appendix Tables A2–A3. Of course, that approximation is arbitrary. Every potential value can be freely selectable on the voltage axes. However, there is no basic point of free selection. Because V_{bi} is obtained by experiment, the choice of V_{bi} is the comparatively accurate approximation. Ref. [4] shows why V_{bi} requires to select.

2.7. Second new serial resistance approximation

Using Eq. (22) let's draw second new serial resistance graphs in the cases of forward bias and reverse bias. In Fig. 4(a) and (b), when graphics examined slopes show like as line-horizontally in both cases. However, each symbol indicates a second new serial resistance value of the slope (see Eq. (22) and in Appendix Tables A1–A3).

Now, let's make the power fitting of the two Metal/n-Si/Al diodes in Fig. 5. Both axes are logarithmic. Resolving knowledge is seen from in Appendix Table A3, respectively. In Fig. 5a the fittings of the diodes have got a negative slope.

2.8. New serial resistances

A symbol is used to represent every first new resistance in the following figures. Each symbol represents to current matching by the V_{bi}. In the both graphs, every slope has six (6) item symbols. R_{Ns1} and R_{Ns2} may comprise R_{s-Ch1} in Appendix Table A1.

2.8.1. First new serial resistance

Fig. 6(a) and (b) shows the first new serial resistance versus the built-in potential. When Fig. 6a was considered, it is seen that each line type has a linear increase. From Fig. 6b, it can be seen that each line type has a linear decrease (see in Appendix Table A1). It is understood that FNSR extended to the negative values in Fig. 6b.
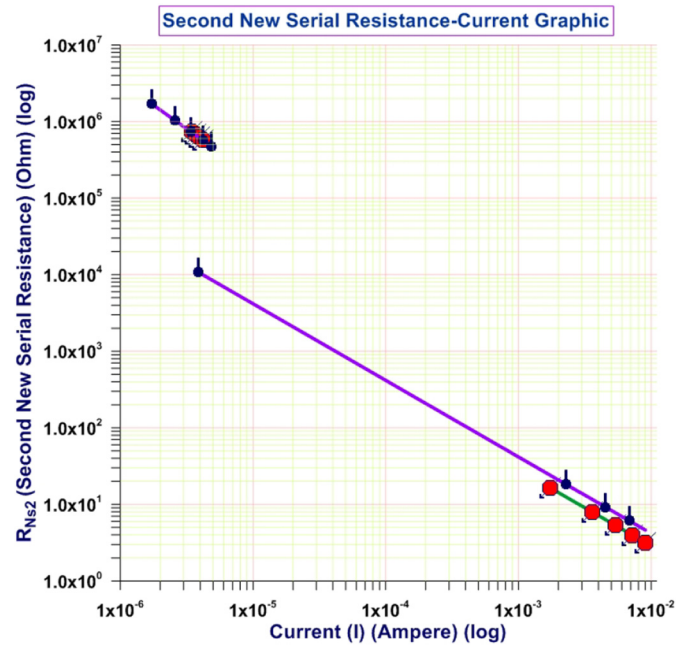

Fig. 5. In the cases of forward bias (down lines) and reverse bias (up lines), R_{Ns2}-I graphics for the two Cu/n-Si/Al (green line), Ag/n-Si/Al (purple line) Schottky diodes (logarithmic R_{Ns2}-log I). (For interpretation of the references to color in this figure legend, the reader is referred to the web version of this article.)

2.8.2. Second new serial resistance

Fig. 7(a) and (b) indicates that SNSR non-linearly decreases for both cases. When Fig. 7(a) and (b) was considered, it can be seen that each line type resembles, except for R_{Ns2-0} (in Appendix Table A3).

2.9. Differential the first new serial resistance and the second serial resistance

When Eq. (23) examined, provided that $\Delta R_{Ns} = R_{Ns1} - R_{Ns2} = [dV / dI]$ is accepted, let's draw ΔR_{Ns}-I plots (which must match I to V_{bi} values) and if ΔR_{Ns} integrates, it gives the
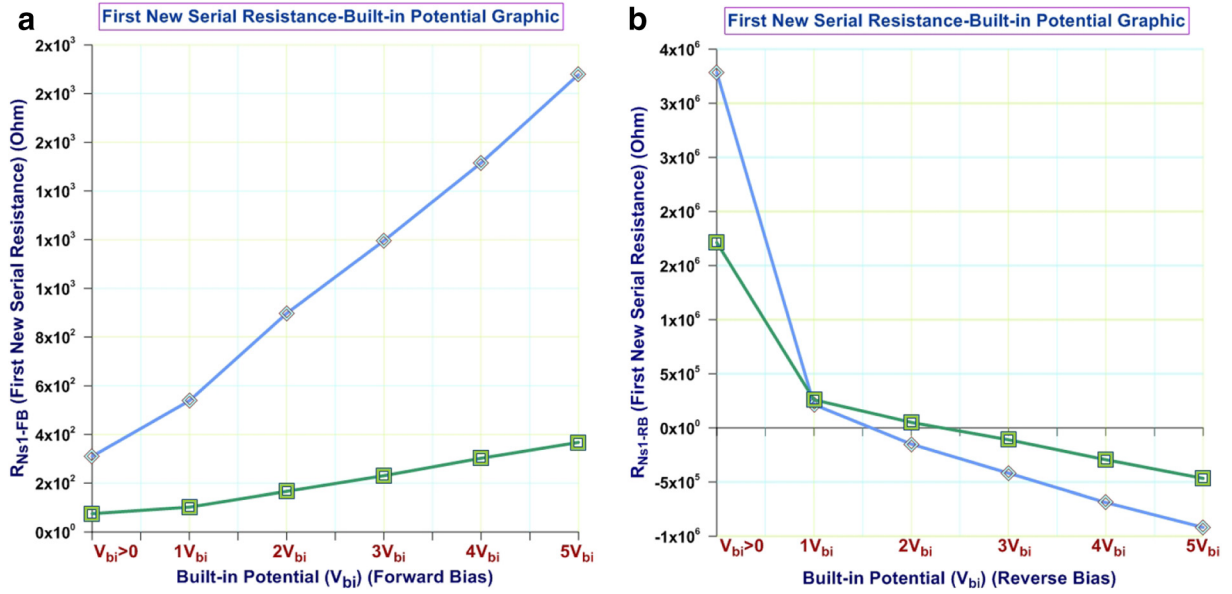
Fig. 6. a) the forward bias, b) the reverse bias; R_{Ns1}–V_{bi} graphics for Cu/n-Si/Al (green line), Ag/n-Si/Al (blue line) Schottky diodes (V_{bi} = 0.386 Volt).
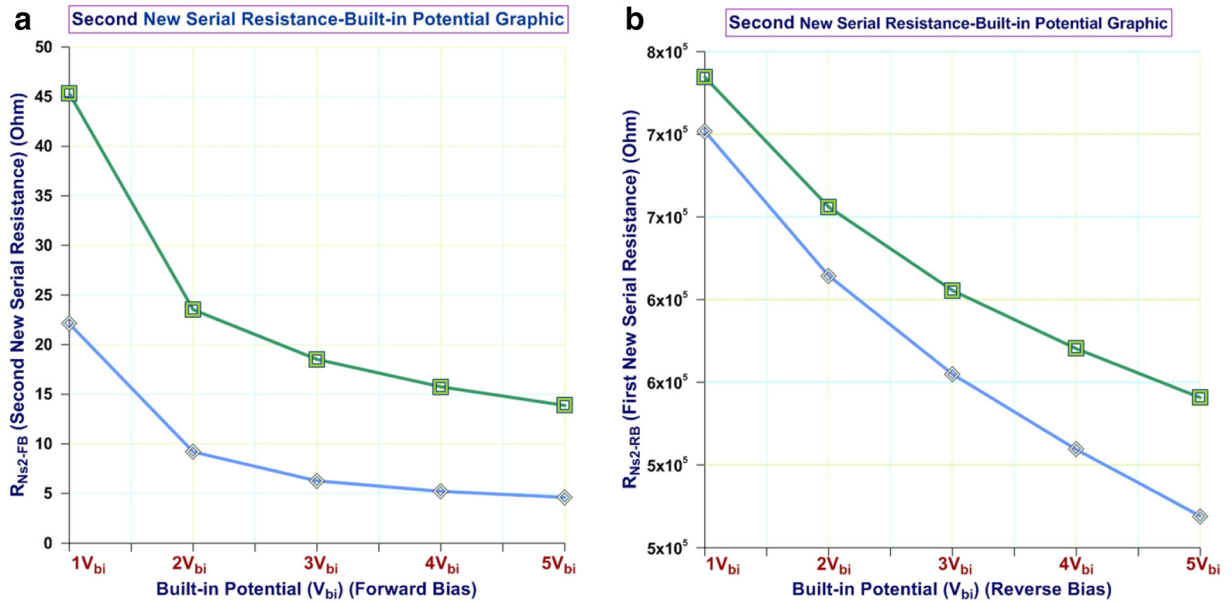

Fig. 7. R_{Ns2}–V_{bi} graphics for Cu/n-Si/Al (green line), Ag/n-Si/Al (blue line) Schottky diodes, a) The forward bias; V_{bi} = 0.386, except for V_a = 0, R_{Ns2} = 559,100 Ω, b) The reverse bias; (V_{bi} = 0.386, except for V_a = 0, R_{Ns2} = 1,697,000 Ω). (For interpretation of the references to color in this figure legend, the reader is referred to the web version of this article.)

following equation,

$$V_{App} = V_{App-0} + (R_{Ns1} - R_{Ns2})(I - I_o) \qquad (26)$$

Fig. 8(a) and (b) shows the plot of differential new serial resistance (DNSR) versus current which is current matching to the V_{bi} values. In the case of reverse bias, it has the absolute value of the ΔR_{Ns}. Following graphs are drawn the Eq. (26) to consider by V_{bi} range (see in Appendix Tables A2–A3) plots.

3. Results

On the contrary to the traditional approach, n_{RB} may be found in the case of reverse bias. The slopes are written in the thermionic equation into Eq. (24). n_{RB} (reverse ideality factor) takes a value higher than n_{FB} (forward ideality factor). In the case of reverse bias, unlike traditional

approximation, serial resistance is obtained from Ch1 equation (see Fig. 2b). Ch1$_{RB}$ value is greater than Ch1$_{FB}$ value.

It was studied on FNSR, SNSR, and R_{s-Ch1} in this work. New equations obtained using Cheung function. The author yields those equations for the first time (Eqs. (8), (9), (10), (22), (23), (26)). The first serial resistance may directly be found from right-side of Eq. (8), where R_{Ns1} = [dV / dI − β_o / I]. Eq. (10) is a general equation resulting in I = I. Eq. (22) is a final equation on serial resistance issue. Then Eq. (26) was obtained. Eq. (26) seems like a "y = ax + b" type in comparison. Indeed, (R_{Ns1}-R_{Ns2}) slope is not constant. Thus, Fig. 9a, b produce the every V_{bi} range.

In Appendix Tables A2–A3, matching current values are given. First V_{bi} has a reference point. The selection of V_{bi} makes it easy [4]. In Ref. [5] Norde's resistance (R = kT/eI$_0$) is mirrored, nevertheless his resistance formula have no ideality factor. The fact remains that his
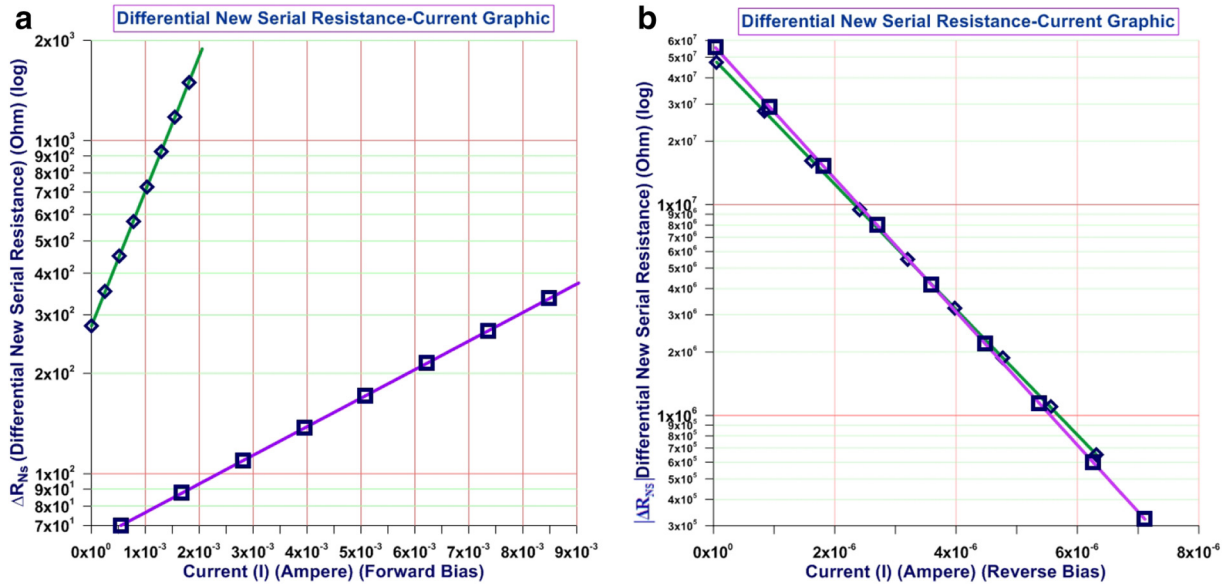
Fig. 8. a) The forward bias, b) the reverse bias; (taking absolute values) ΔR_{Ns} –I graphics for Cu/n-Si/Al (green line), Ag/n-Si/Al (purple line) Schottky diodes. (For interpretation of the references to color in this figure legend, the reader is referred to the web version of this article.)

Norde's resistance values [5] are almost identical to ours (see Fig. 1 p. 5052). In Ref. [13] authors found dependency on voltage using a resistance formula values which are almost identical to ours (see Fig. 1 p. 093505-2). In Ref. [14] Lambert function has R_{Ns2}, however it does not contain minus (p.024502-6). In Ref. [15], Eq. (4) has R_{Ns2}, whereas it includes no minus (p. 10076).

4. Conclusion

New serial resistances were obtained by differentiating the Cheung functions. New serial resistance formulae result in very exceptional serial resistance value for both cases, the forward bias and the reverse bias. The two new serial resistance equations (i.e., R_{Ns1} and R_{Ns2}) exhibit a stable behavior. Also, another advantage might be scanning the all current and voltage values in a specific range depending on the built-in potential. The stable serial resistance values could be derived from new serial resistance formulae. Besides, R_{Ns}-I graph could be easily plotted to use current values coming up to the built-in potential values. It is enough to take matching current the built-in potential integer values [4]. Matching current value on V_{bi} is very useful; otherwise, it will require further trials with too much data. In Figs.4, 7 a general view is presented on new serial resistance of the metal/n-Si/Al diodes. The Eqs. (9), (22), (23) and (26) represent new serial resistance approximation. Those examples are Ag/n-Si/Al, and Cu/n-Si/Al, respectively, (D1 and D2). R_{Ns1} and R_{Ns2} may comprise by R_{s-Ch1}. R_{Ns2} is less than R_{Ns1}. R_{Ns2} method is found to be easier than R_{s-Ch1} method. Besides, R_{Ns2} has a starting point like as V_{bi}. It is not necessary to take derivation of a function, as seen in Ch1. Therefore, the new method has got too many gains. Those new equations may be considered as a new Schottky contact characteristic. How should minus sign of R_{Ns2} be understood?
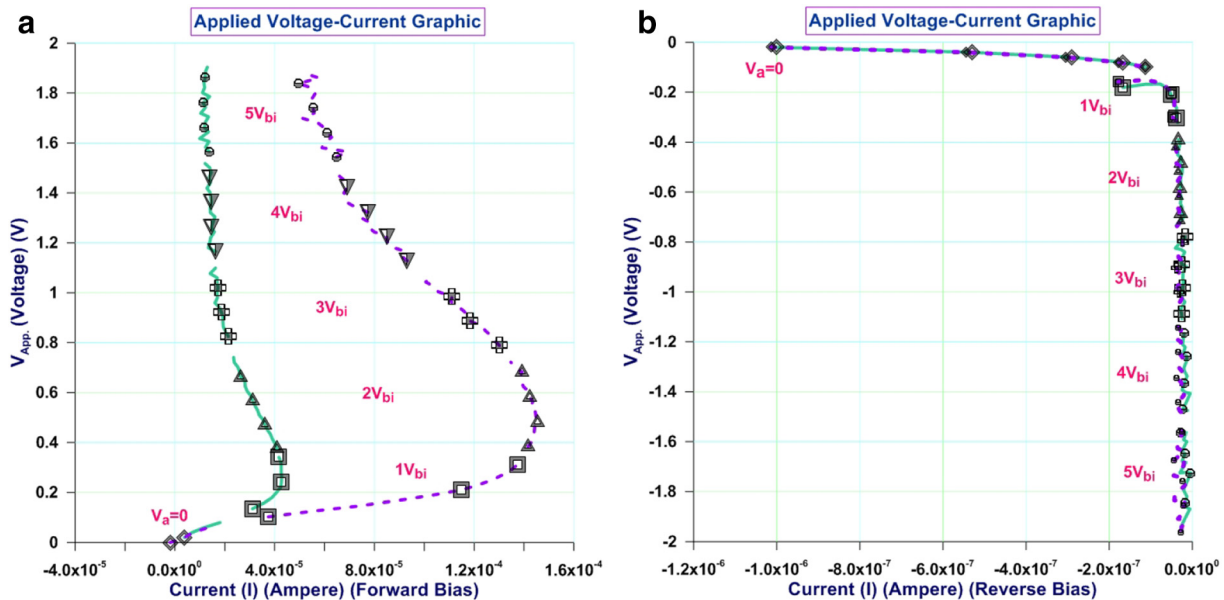

Fig. 9. a) The forward bias, b) the reverse bias, V_{app} -I graphic for Cu/n-Si/Al (green line), Ag/n-Si/Al (purple dashed line) Schottky diodes (line type: diamond; $V_a = 0$, square; V_{bi}, triangle; $2 \times V_{bi}$, plus; $3 \times V_{bi}$, triangle; $4 \times V_{bi}$, circle; $5 \times V_{bi}$), (For interpretation of the references to color in this figure legend, the reader is referred to the web version of this article.)

The minus sign may indicate that the diode layers put up less resistance to the electric counter-current in the case of forward bias. Total resistance is the little. The diode layers put up extra resistance to the electric counter-current in the case of reverse bias. Total resistance is high. This case is so reasonable that the diode device has to conduct the one way (to the forward bias) and it also has a little resistance; namely, the diode is in the "on" state, diode conduct electric current. Otherwise, if diode has an extra resistance, the diode is in the case of reverse bias, and it conduct no electric current; namely, the diode is in the "off" state

(in Appendix Table A1). Eq. (23) always gives us a minimum value, $R_{s\text{-}min}$ and a maximum value, $R_{s\text{-}max}$ as shown Norde's article [5], however Norde method is ineffective to foresee a maximal resistance in both cases (FB and RB).

Acknowledgment

Appendix A

Table A1
$n_{IV\text{-}FB/RB}$ and $R_{s\text{-}Ch1\text{-}FB/RB}$ values of Metal/n-Si/Al Schottky diodes.

Diode symbol	Diodes	Ideality factor ($n_{IV\text{-}FB}$)	Ideality factor ($n_{IV\text{-}RB}$)	Serial resistance (Ω) $R_{s\text{-}Ch1\text{-}FB}$	Serial resistance (Ω) $R_{s\text{-}Ch1\text{-}RB}$
D1	Ag/n-Si/Al	1.061	−129.048	147.428	1,182,492.115
D2	Cu/n-Si/Al	1.103	−145.844	577.190	1,359,642.318

Table A2
$R_{Ns1\text{-}FB/RB}$ values from Fig. 3a, b.

D1; Ag/n-Si/Al	The forward bias; RNs1-1…6; $\ln(Y) = 160.8033675 * X + 4.434670578$		The reverse bias; RNs1-1…6; $Y = -3.079658404E + 011 * X + 1,723,077.625$	
Vbi (Volt)	I (Ampere)	(RNs1-FB) (Ω)	I (Ampere)	(RNs1-RB) (Ω)
0	3.231873E − 008	84.324	3.231873E − 08	1.713125E + 6
0.386	0.001739406	111.538	4.753696E − 06	2.591016E + 5
0.772	0.004527651	174.640	5.429783E − 06	5.088994E + 4
1.12	0.006558201	242.075	6.012423E − 06	− 1.285433E + 5
1.544	0.007925039	301.582	6.550170E − 06	− 2.941510E + 5
1.92	0.00898007	357.342	7.085544E − 06	− 4.590279E + 5
D2; Cu/n-Si/Al	The forward bias; RNs1-1…6; $\ln(Y) = 916.8576749 * X + 5.657905013$		The reverse bias; RNs1-1…6; $Y = -6.715920927E + 011 * X + 3,319,900.771$	
Vbi (Volt)	I (Ampere)	(RNs1-FB) (Ω)	I (Ampere)	(RNs1-RB) (Ω)
0	5.099819E − 08	286.561	5.099819E − 008	3.285651E + 6
0.386	0.00062942	510.300	4.623406E − 006	2.148579E + 5
0.772	0.00121207	870.615	5.166421E − 006	− 1.498267E + 5
1.12	0.00153976	1175.740	5.613684E − 006	− 4.502050E + 5
1.544	0.00180998	1506.292	5.968819E − 006	− 6.887109E + 5
1.92	0.00205499	1885.670	6.298257E − 006	− 9.099588E + 5

Table A3
$R_{Ns2\text{-}FB/RB}$ values from Fig. 4a, b.

D1; Ag/n-Si/Al	The forward bias; $R_{Ns2\text{-}1…6} = \exp(Y)$ $\ln(Y) = -1.000005564 * \ln(X) - 3.596179539$		The reverse bias; $R_{Ns2\text{-}1…6} = \exp(Y)$ $\ln(Y) = -0.9999732709 * \ln(X) + 1.205119124$	
V_{bi} (Volt)	I (Ampere)	($R_{Ns2\text{-}FB}$) (Ω)	I (Ampere)	($R_{Ns2\text{-}RB}$) (Ω)
0	3.231873E − 008	8.488E + 5	3.231873E − 08	1.032E + 8
0.386	0.001739406	15.769	4.753696E − 06	7.018E + 5
0.772	0.004527651	6.058	5.429783E − 06	6.144E + 5
1.12	0.006558201	4.182	6.012423E − 06	5.549E + 5
1.544	0.007925039	3.461	6.550170E − 06	5.093E + 5
1.92	0.008980070	3.054	7.085544E − 06	4.708E + 5
D2; Cu/n-Si/Al				

A. Korkut

Microelectronic Engineering 197 (2018) 45–52

Table A3 (*continued*)

D1; Ag/n-Si/Al	The forward bias; $R_{Ns2\text{-}1\ldots6} = \exp(Y)$ $\ln(Y) = -1.000005564 * \ln(X) - 3.596179539$		The reverse bias; $R_{Ns2\text{-}1\ldots6} = \exp(Y)$ $\ln(Y) = -0.9999732709 * \ln(X) + 1.205119124$	
V_{bi} (Volt)	I (Ampere)	$(R_{Ns2\text{-}FB})$ (Ω)	I (Ampere)	$(R_{Ns2\text{-}RB})$ (Ω)
	The forward bias; $R_{Ns2\text{-}1\ldots6} = \exp(Y)$ $\ln(Y) = -0.9999884239 * \ln(X) - 3.557282874$		The reverse bias; $R_{Ns2\text{-}1\ldots6} = \exp(Y)$ $\ln(Y) = -1.000109959 * \ln(X) + 1.227323916$	
V_{bi} (Volt)	I (Ampere)	$(R_{Ns2\text{-}FB})$ (Ω)	I (Ampere)	$(R_{Ns2\text{-}RB})$ (Ω)
0	5.099819E−08	5.591E+5	5.099819E−008	6.703E+7
0.386	0.00062942	45.301	4.623406E−006	7.390E+5
0.772	0.00121207	23.525	5.166421E−006	6.613E+5
1.12	0.00153976	18.518	5.613684E−006	6.086E+5
1.544	0.00180998	15.754	5.968819E−006	5.724E+5
1.92	0.00205499	13.876	6.298257E−006	5.425E+5

References

[1] S.K. Cheung, N.W. Cheung, Extraction of Schottky diode parameters from forward current-voltage characteristics, Appl. Phys. Lett. 49 (2) (1986) 85.

[2] K. Sreenu, C.V. Prasad, V.R. Reddy, Barrier parameters and current transport characteristics of Ti/p-lnP Schottky junction modified using Orange G (OG) organic interlayer, J. Electron. Mater. (2017), http://dx.doi.org/10.1007/s11664-017-5611-9.

[3] S.M. Sze, Physics of Semiconductor Devices, J, Wiley&Sons, Singapore, 1981.

[4] A. Korkut, Differential depletion capacitance approximation analysis under DC voltage for air-exposed cu/N-Si Schottky diodes, Surf. Rev. Lett. 25 (4) (2017) 1850043, , http://dx.doi.org/10.1142/S0218625X18500439.

[5] H. Norde, A modified forward I-V plot for Schottky diodes with high series resistance, J. Appl. Phys. 50 (1979) 5052, http://dx.doi.org/10.1063/1.325607.

[6] M.K. Hudait, S.B. Kurupanidhi, Interface states density distribution in Au/n-GaAs Schottky diodes on n-Ge and n-GaAs substrates, Mater. Sci. Eng. B87 (2001) 141.

[7] M.K. Hudait, S.B. Kurupanidhi, Effects of thin oxide in metal/semiconductor and metal/insulator/semiconductor epi-GaAs Schottky diodes, Solid State Electron. 44 (2000) 1089.

[8] K.K. Ng, Complete Guide to Semiconductor Devices, McGraw-Hill Inc., Newyork, 1995.

[9] B.L. Sharma, Metal-Semiconductor Schottky Barrier Junctions and Their Applications, Plenum Press, UK, 1984.

[10] M. Shur, Physics of Semiconductor Devices, Prentice-Hall Inc., New Jersey, 1990.

[11] D.K. Schroder, Semiconductor Material and Device Characterization, J, Willey& Sons, USA, 2006.

[12] E.H. Rhoderick, R.H. Williams, Metal–Semiconductor Contacts, Clarendon Press, Oxford, 1988.

[13] H. Durmuş, Ülfet Atav, Extraction of voltage-dependent series resistance from I-V characteristics of Schottky diodes, Appl. Phys. Lett. 99 (2011) 093505, , http://dx.doi.org/10.1063/1.3633116.

[14] O.Y. Olikh, Review and test of methods for determination of the Schottky diode parameters, J. Appl. Phys. 118 (2015) 024502, , http://dx.doi.org/10.1063/1.4926420.

[15] R.M. Cibils, R.H. Buitrago, Forward I-V plot for nonideal Schottky diodes with high series resistance, J. Appl. Phys. 58 (1985) 1075, http://dx.doi.org/10.1063/1.336222.

View publication stats